不同应力状态下局部材料损伤行为

车洪艳[1,2]， 陈剑虹[1,2]， 朱 亮[1,2]， 吕先锋[1,2*]
（1. 兰州理工大学 材料科学与工程学院，兰州 730050；
2. 兰州理工大学 甘肃省有色金属新材料省部共建国家重点实验室，兰州 730050）

摘 要：为研究局部材料在不同应力状态下的变形及损伤行为，进行双孔微剪切试验。选取两组试样，试样厚度均为 1 mm，试样 1 双孔直径均为 2 mm，孔间距为 0.4 mm；试样 2 与试样 1 相比，改变其中一个孔径的尺寸，使其为试样 1 孔径的 2 倍，并减小两孔之间小桥的间距，使其为试样 1 间距的一半。选用铝合金 6063 为研究对象，应用 ABAQUS/Explicit 结合 Gurson 损伤模型模拟材料在两种应力状态下的变形及损伤行为。结果表明，Gurson 模型较好地预测了试样 2 的损伤行为，说明试样 2 在不同于试样 1 的应力状态下损伤，分析原因，试样 2 在材料损伤之前三向应力度大于 0.4，Gurson 模型适合于模拟三向应力度较高的情况。

关键词：铝合金；双孔试验；损伤；有限元
中图分类号：TG1462 文献标识码：A 文章编号：0253－360X(2008)11－0073－04

车洪艳

0 序 言

汽车在碰撞过程中部件要经历较大的塑性变形，进而材料将发生损伤，直至断裂，在此过程中部件中的焊接接头由于各区的性能不均匀因而材料的变形及损伤行为变得更加复杂。有限元仿真已经成为一种重要的研究方法，为提高模拟的精度，需要准确获得局部材料的性能参数[1,2]。然而焊缝及热影响区由于尺寸的限制不能通过常规的拉伸试验获得这些参数，在文献[3]的研究中，应用双孔微剪切试验与有限元仿真相结合能够较准确得到局部材料的性能参数，并应用宏观现象学的 Johnson-cook 损伤模型预测局部材料在剪切应力状态下的损伤行为。而部件在碰撞的过程中，焊接接头部位由于焊缝及热影响区的存在，应力状态更加复杂。为研究带有焊缝的部件变形及损伤行为，首先要准确表征焊缝及热影响区这些区域在不同应力状态下的变形及损伤行为，作者在文献[3]的基础上，选用铝合金 6063 为研究对象，改变孔径及双孔之间距离，进行试验，对比不同的试验结果，应用 ABAQUS/Explicit 进行有限元模拟，并应用 Gurson 模型预测材料的损伤行为。

收稿日期：2008－01－14
基金项目：国家重大基础研究前期研究专项(2004CCA04900)
*参加此项研究工作的还有徐文福

1 试 验

1.1 试验原理

首先在试样上选定被测材料区域，在第一组被测试样(试样 1)的两侧分别钻直径为 2 mm 的两个通孔，孔间距为 0.4 mm，孔间的小桥为被测量区域，为了保证试验数据的可靠性，在一块试板上打 5 组这样的通孔，每组间隔 5 mm 以上；第二组被测试样(试样 2)改变孔径在两侧分别钻直径为 2 mm 和 4 mm 的两个通孔，孔间距为 0.2 mm。试验原理见图 1，孔的分布及孔的具体尺寸见图 2。

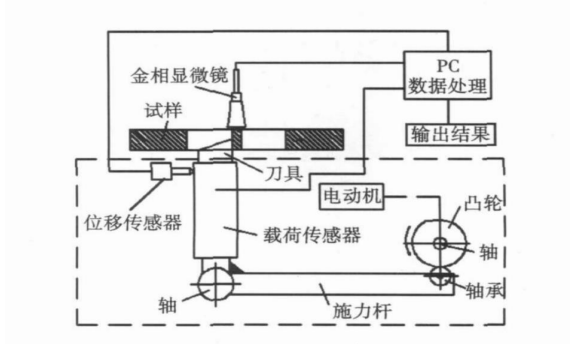

图 1 试验原理图

Fig. 1 Test principle

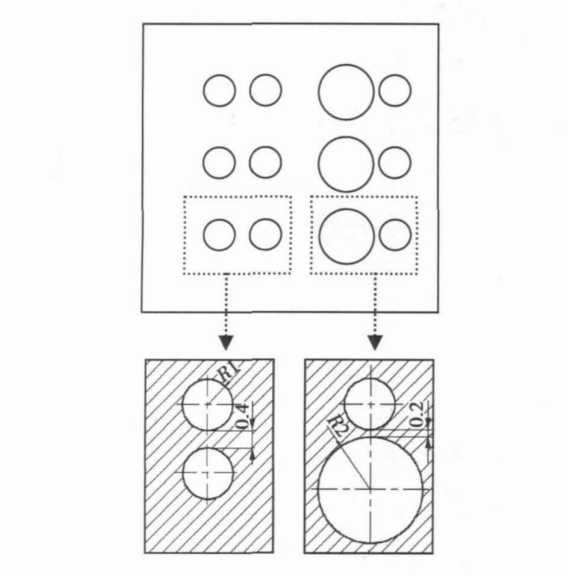

图 2 试样形状及尺寸

Fig. 2 Configuration and dimensions of specimen

1.2 试验过程及结果

试验采用 6063 铝合金为研究对象，通过改变孔径大小及两孔之间的距离来实现局部材料在不同的应力状态下破坏。采用电动机带动传力杆在双孔的小桥之间施加向前的载荷（图 1），载荷传感器记录所加的电压，位移传感器靠近刀头位置以便准确测量刀头的位移。将此装置与自动记录装置连接，得到力和变形的曲线。试验在室温下进行，加载速度为 1 mm/min，试验的载荷位移曲线如图 3 所示。

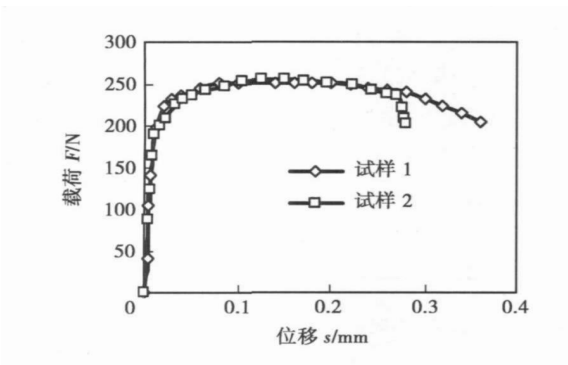

图 3 双孔试验的载荷位移曲线

Fig. 3 Result of double-hole

2 有限元模拟

2.1 有限元模型的建立

为了提高模拟结果的准确性，试样以三维实体建模。刀头采用分析刚体建模，装配好的模型如图 4a 所示。左右两个边界限制 1，3 方向的位移和 1，2，3 方向的旋转，下边界限制 1，2，3 三个方向的位移和旋转，上边界自由，刀头限制 1，3 方向的位移及 1，2，3 方向的旋转。为了提高计算精度在小桥连接处细化网格，单元尺寸为 0.02 mm，类型为 C3D8R，试样 1 的网格划分如图 4b 所示。

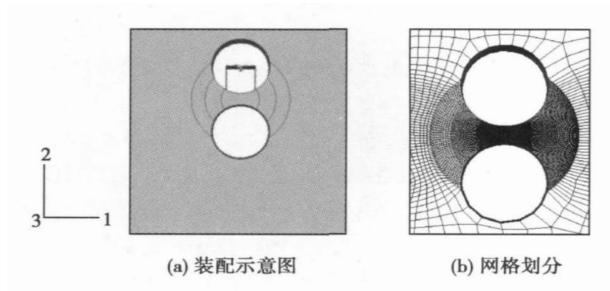

图 4 试样 1 的装配示意图及网格划分

Fig. 4 Assembling and mesh size of sample 1

材料的损伤模型参数通过有限元反推法从拟合平板拉伸试验中获得，因为损伤参数与单元尺寸相关，因此应用调节后的损伤参数对双孔试验进行模拟[4]。

2.2 Gurson 损伤模型

1975 年 Gurson 在 McClintock，Rice 和 Tracey 等工作基础上发展了一套比较完整的本构方程，用以描述微孔洞损伤对材料塑性变形行为的影响[5]。在 ABAQUS/Explicit 中 Gurson 模型的失效准则为

$$\phi = \left(\frac{q}{\sigma_y}\right)^2 + 2q_1 f^* \cosh\left(-q_2 \frac{3p}{2\sigma_y}\right) - (1 + q_3 f^{*2}) = 0 \tag{1}$$

式中：q 为等效 Mises 应力；p 为静水压力；σ_y 为屈服应力；q_1，q_2，q_3 为材料参数；f^* 为

$$f^* = \begin{cases} f & f \leqslant f_c \\ f_c + \dfrac{f_F - f_c}{f_F - f_c}(f - f_c) & f_c < f < f_F \\ f_F & f \geqslant f_F \end{cases} \tag{2}$$

式中：f_c 为孔洞体积分数的临界值；f_F 为断裂时的孔洞体积分数。f_F 为

$$f_F = \frac{q_1 + \sqrt{q_1^2 - q_3}}{q_3} \tag{3}$$

在 Gurson 模型中，损伤被视为各向同性，损伤变量用一个标量即孔洞体积百分比来表示，因为对于韧性金属来说，损伤引起的各向异性往往不是非常明显。孔洞体积分数的演化包括两部分，即

$$f = f_{gr} + f_{nucl} \tag{4}$$

式中：f_{gr} 为孔洞长大引起的孔洞体积分数的变化率；f_{nucl} 为新孔洞形核所引起的孔洞体积分数变化率。

$$f_{gr} = (1-f)\varepsilon^{pl} : I \tag{5}$$

$$f_{nucl} = A\dot{\varepsilon}_m^{pl} \tag{6}$$

$$A = \frac{f_N}{S_N \times \sqrt{2\pi}} \exp\left[-\frac{1}{2}\left(\frac{\bar{\varepsilon}_m^{pl} - \varepsilon_N}{S_N}\right)^2\right] \tag{7}$$

式中：ε_N 为孔洞形核的平均应变；S_N 为相应的标准方差；f_N 为可以发生微孔洞形核的所有二相粒子的体积百分比；ε^{pl} 为塑性应变率；$\dot{\varepsilon}_m^{pl}$ 为矩阵的塑性应变率；$\bar{\varepsilon}_m^{pl}$ 为矩阵的等效塑性应变。

3　结果及讨论

3.1　断口观察

试样断口形貌如图 5 所示。

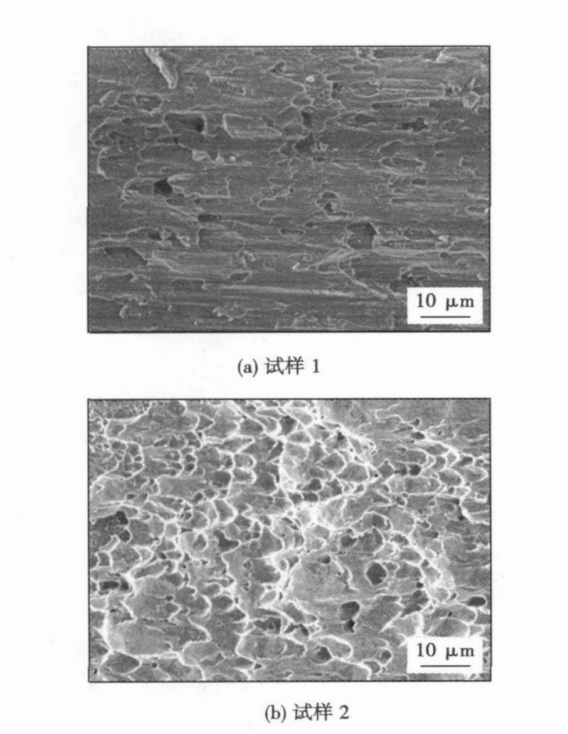

图 5　断口形貌

Fig. 5　Fracture surfaces from two tests

从图 5 中可以看出，试样 1 的韧窝呈抛物线形，在剪切应力的作用下显微孔洞沿剪切方向被拉长。试样 2 的韧窝明显比试样 1 增多，且韧窝的深度有所增加，韧窝大量聚集在断口上，说明在正应力的作用下，孔洞在空间三个方向上长大。相对于试样 1，应力状态已经发生改变。

3.2　试验结果及有限元仿真

应用 Gurson 损伤模型模拟双孔试验时材料的损伤行为，试验与仿真结果的载荷—位移曲线如图6所示。

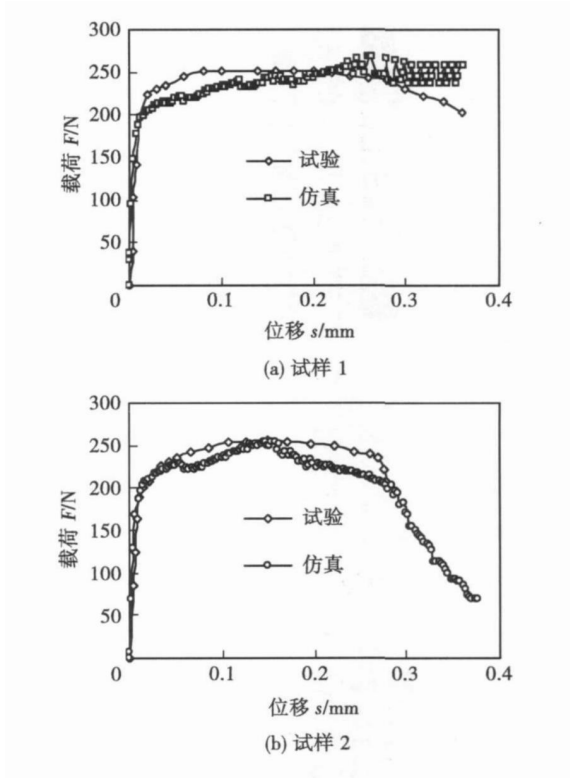

图 6　试验和仿真的对比曲线

Fig. 6　Comparison of test and simulation

从图 6a 中可以看出，仿真与试验结果吻合的不是很好，而图 6b 显示 Gurson 模型较好地预测了材料的损伤行为。图 7 为在损伤发生的前一个增量步，材料单元的三向应力度与等效塑性应变的关系。其中仿真 1 是对试验 1 的仿真结果，仿真 2 是对试验 2 的仿真结果。从图中可以看出仿真 1 中三向应力度小于 0.3，仿真 2 中三向应力度大于 0.4，说明试样 2 在拉应力的作用下破坏。图 8 为不同试样仿真结果的 Mises 应力对比图，两个仿真结果显示在与刀头相接触的位置上试样表面的 Mises 应力都比较集中，但对于仿真 2 在小桥底部 Mises 应力也比较集中，如图 8b 中 A 点所示。

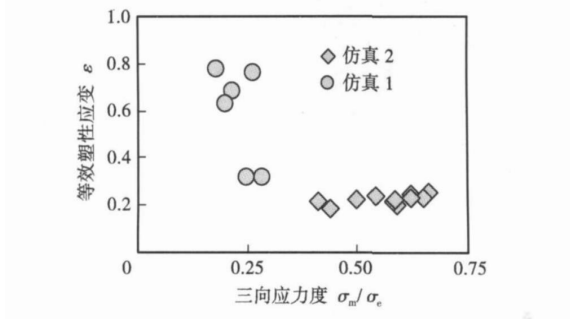

图 7　三向应力度与等效塑性应变

Fig. 7　Comparison on triaxial stress under different test condition

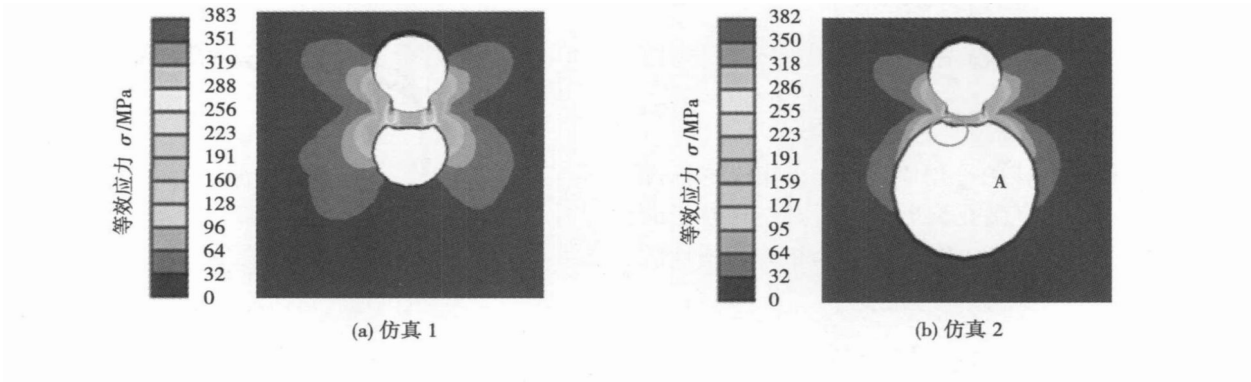

图 8 Mises 分布

Fig. 8 Distribution of Mises

图9 为损伤单元消去后不同试验仿真结果的对比。图片局部放大, 从图 9 中可以看出, 在对试验 1 的仿真中, 单元在与刀头相接触的两侧首先发生损伤, 损伤的演化沿着与剪切面成一定角度扩展, 这和

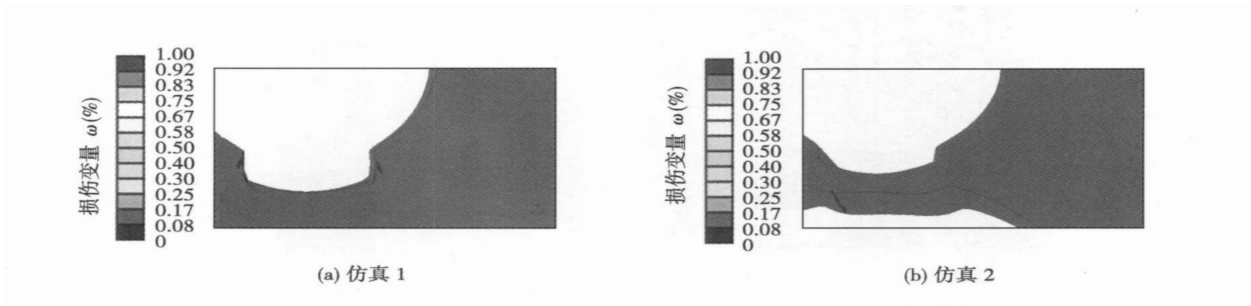

图 9 损伤单元消去后结果

Fig. 9 Result of simulation

文献[3] 的研究结果基本吻合, 而对于仿真 2, 单元在小桥的底部首先损伤, 此处正是受拉应力最大的部位, 裂纹沿着与小桥垂直的方向扩展, Gurson 模型很好地预测了材料的损伤行为。

4 结 论

(1) 与不改变孔径及小桥间距相比, 改变孔径后的试样, 在拉应力作用下于小桥底部发生损伤。

(2) 应用微观机理的 Gurson 损伤模型较好地预测了材料在拉应力作用下的损伤行为。材料单元在损伤前的三向应力度分布在 0.4 ~ 0.7 之间。说明通过双孔试验可以实现局部材料在不同的应力状态下变形及损伤行为, 为进一步在焊缝和热影响区进行研究奠定了基础。

参考文献:

[1] Haug Eberhard, Clinckemaillie Jan, 宁小敏. 汽车碰撞仿真设计的最新进展和发展趋势[J] . 机械工程学报, 1998, 34(1): 93－99.

[2] Kim Y J, Schwalbe K H. Mismatch effect on plastic yield loads in idealised weldments: ⅡHeat affect zone cracks [J] . Engineering Fracture Mechanics, 2001, 68(2): 183－199.

[3] 车洪艳, 朱 亮, 陈剑虹. 局部材料损伤行为的双孔微剪切实验[J] . 兰州理工大学学报, 2007, 33(4): 31－34.

[4] 车洪艳, 朱 亮, 陈剑虹. 有限元反推法评定 AA6014 铝合金的损伤参数[J] . 机械工程材料, 2007, 31(7): 57－59.

[5] 余寿文, 冯西桥. 损伤力学[M] . 北京: 清华大学出版社, 1997.

作者简介: 车洪艳, 女, 1977 年出生, 博士研究生。主要从事铝合金汽车部件的碰撞仿真研究。发表论文 7 篇。

Email: earlyautumn@sina.com.cn

tially. The research results can provide the possibility on optimizing welding procedure of high temperature pipe and controlling welding residual stress effectively.

Key words: high temperature pipe; orthogonal experiment design; welding procedure; optimization; numerical simulation

A novel ultrafast-convert complex-pulse variable-polarity arc welding power topology QI Bojin, CONG Baoqiang (School of Mechanical Engineering and Automation, BeiHang University, Beijing 100083, China). p57—60

Abstract: A novel main circuit topology of ultrafast-convert complex high-frequency pulse square-wave variable-polarity arc welding power supply was designed and analyzed, which consisted of two parts. In the front part, the base current and pulse current were provided by two independent direct-current power supplies. In the latter part, direct current was transformed into series of high-frequency complex-pulse variable-polarity current, which crosses zero with no dead-time, by high-frequency pulse-forming circuit and full-bridge current-polarity transform circuit. The reliability and safety of the circuit system was effectively provided by assistant parallel-connection protecting circuit. The results of aluminum alloy variable polarity tungsten inert-gas welding show that the high-frequency complex-square-wave variable polarity current generated by novel circuit topology has fast rising and falling edge, which can satisfy the requirements of a novel high-strength and high-efficiency special variable polarity arc welding.

Key words: ultrafast convert; complex high-frequency pulse; variable-polarity square-current

Effect of elements diffusion behavior on thermal fatigue of nickel based alloy coating deposited with thermal spraying CHEN Yajun[1,2], WANG Zhiping[2], JI Zhaohui[2], DING Kunying[2], WANG Lijun[1] (1. School of Materials Science and Engineering, Tianjin University, Tianjin 300072, China; 2. College of Sciences, Civil Aviation University of China, Tianjin 300300, China). p61—64

Abstract: Thermal spraying technique was applied to produce nickel based alloy coating on Cu alloy. Optical microscope, SEM analysis were used to investigate the elemental diffusion and the microstructure in the interface between the nickel based alloy coating and the substrate. And the influence of the elements diffusion behavior on thermal fatigue resistance was studied. The results show that alloy elements distribute continuously from nickel based alloy coating to substrate, and have an abrupt change at the interface between the substrate and coating. During heat treatment, an inter-diffusion layer appears between the substrate and coating, and the ability of Cu element diffusion was improved with the increase of temperature and time. The main affecting factor was temperature, and the effect of time was followed during heat treatment. The thermal fatigue resistance of nickel based alloy coating was improved by elements diffusion. The thermal spraying coating endured 85 time thermal shock at 550 ℃ was perfect without defects such as crack and spalling.

Key words: thermal spraying; nickel based alloy coating; diffusion behavior; thermal fatigue

Space welding seam tracking beased on free floating space robot GAO Sheng, CHANG Yulian, ZHANG Ruijie, REN Yongliang (School of Mechanical Science and Engineering, Daqing Petroleum Institute, Daqing 163318, Heilongjiang, China). p65—68

Abstract: Space robot can fly or float in the space to help or replace astronauts to perform space welding task. For a planar free floating dual-arm space robot, the path planning of welding torch position and configuration in tracking space weld is studied. On the basis of kinetic model of dual-arm space robot, the computational approach of robot arm end velocity is discussed and analyzed, and the solution of dual-arm end velocity is defined as a multi-dimentional searching problem, which is solved by introducing Genetic Algrithom to optimize calculation parameter. Finally, an algrithom of path planning of dual-arm space robot tracking space weld is proposed, which is verified and analyzed by two simulation experiments of line and arc welding seam tracking.

Key words: space robot; motion planning; weld; tracking

Analysis on dynamic resistance in resistance spot welding of stainless steel WEN Jing[1], WANG Chunsheng[2], XU Guocheng[1], CHENG Guoli[2] (1. School of Materials Science and Engineering, Jilin University, Changchun 130025, China; 2. Changchun Railway Vehicles Corporation, Changchun 130062, China). p69—72

Abstract: The dynamic resistance signal was collected by an automatic data acquisition system. Research indicated that the dynamic resistance signal responded well to the change of welding parameters, and contained plenty of quality information. There was an obvious correspondence between the dynamic resistance signal and the growth process of nugget. The inflexion time and destination value of dynamic resistance curve had strong relativity with the time of nugget appearance and the final size of the nugget respectively. Welding parameters affected the dynamic resistance signal obviously and regularly. When an expulsion occurred, a sharp drop in dynamic resistance curve and a peak in the change rate of dynamic resistance curve can be used to automatically identify the splash.

Key words: stainless steel; resistance spot welding; dynamic resistance

Damage behavior within local materials at different stress states CHE Hongyan[1,2], CHEN Jianhong[1,2], ZHU Liang[1,2], LV Xianfeng[1,2] (1. College of Materials Science and Engineering, Lanzhou University of Technology, Lanzhou 730050, China; 2. State Key Laboratory of Gansu Advanced Non-ferrous Metal Materials Lanzhou University of Technology, Lanzhou 730050, China). p73—76

Abstract: In order to study the damage behavior within local materials at different stress state, two kinds of doble-hole tests were carried out. The thickness of the specimen is 1 mm. The radius of hole are same in the first specimen. However, the radius of hole are

different in the second specimen. One of them is 1 mm, and the other one is 2 mm. Meanwhile, the size of bridge between two hole are different. The former is 0.4 mm, and the later is 0.2 mm. Then the numerical resultes were compared with that of the experiment to verify the validity of Gurson damage models in describing the initiation and propagation of cracks during their evolution. The results show Gurson damage model give good results to the second specimen. Because the stress triaxiality of second specimen greater than 0.4.

Key words: aluminium alloy; double-hole test; damae; finite element method

Wear resistance of chromium carbides coating alloyed by vacaum electron beam LU Binfeng, LU Fenggui, TANG Xinhua, YAO Shun (Shanghai Key Laboratory of Materials Laser Processing and Modification, Shanghai Jiaotong University, Shanghai 200240, China). p77—80

Abstract: Fe/Cr/C powder mixtures were employed to modify the surface of a low carbon steel substrate by electron beam irradiation in vacuum condition. By optimizing the electron beam parameters, chromium carbide is in situ synthesized in the surface composite layer. The surface composite layer was analyzed with optical microscope, XRD analysis and trobological test. There are two main phases in the surface composite layer: chromium carbides as hard phase and austenite as tough phase. There are little typical hexagonal primary chromium carbides in the surface composite layer. Eutectic chromium carbides dispersively distribute between the interface of austenite phase to form a net like structure. It is metallurgical combination in the surface composite layer and the substrate. The existing of carbides in the composite layer provides a notable improvement on the wear resistant property of the surface layer.

Key words: surface composite layer; vacuum electron beam irradiation; chromium carbide; wear resistance

Offline automatic programming of arc prototype system based on arc welding robot DU Naicheng[1,2], HU Shengsun[1,2], DING Wei[1] (1. School of Materials Science and Engineering, Tianjin University, Tianjin 300072, China; 2. Tianjin Key Laboratory of Advanced Joining Technology, Tianjin university, Tianjin 300072, China). p81—84

Abstract: At present, methods of graphic teaching for robot are mostly adopted in offline programming system to establish the path of robotic movement. However, for this programming of the approach complex path, the workload is still a large. Moreover, the robot procedure (JOB) is hardly formed by using the position data and welding instructions, which calculated directly by path planning. The offline automatic programming was researched for arc welding robots. The relative JOB is a data exchange interface of MOTOMAN robots. With this interface, the offline automatic programming module generates robots procedures. Through ODBC interface, offline automatic programming module queries the planning instructions and data in the corresponding database in the arc prototype system. The advantages of database are conducive to the expansion of offline programming system. The experiment results show that the researched offline programming operates stably, and the robot moves coherently, and the welding path is accordant to the design.

Key words: robot; arc prototype; offline automatic programming; relative job

Quantitative analysis method of geometrical precision quality on precision welding structure KONG Liang[1], YU Hailiang[1], JIN Xin[1], WU Yixiong[1,2] (1. School of Materials Science and Engineering, Shanghai Jiatong University, Shanghai 200030, China; 2. Shanghai Key Laboratory of Materials Laser Processing and Modification, Shanghai Jiaotong University, Shanghai 200240, China). p85—88

Abstract: Based on fussy set theory, a quantitative method for welding geometrical quality control of precision welding structure (PWS) is presented. The "Quality Differentiation Coefficient" which characterizes the relation between quality difference and effective quality essentials is adopted to formulate the qualitative linguistic variables of welding quality difference properties. The welding quality analysis model which could fully utilize experts experiments and historical data for PWS is established to quantificational analysis and decision-making.

Key words: precision welding structure; welding geometrical precision; quantification; quality analysis

Misalignment production and its prediction model in tailored blank laser welding XIN Liming[1,2], ZHAO Mingyang[1], XU Zhigang[1] (1. Shenyang Institute of Automation, Chinese Academy of Science, Shenyang 110016, China; 2. Graduate School of the Chinese Academy of Sciences, Beijing 100039, China). p89—92, 96

Abstract: Misalignment is an important quality evaluation standard in tailor welded blanks. The control of misalignment, especially for thinner blanks, is a difficult problem in tailored blank laser welding process. The production and control of misalignment is studied based on a tailored blank laser welding system. The influential factors of the misalignment are obtained after numbers of experiments: the deformation of the blanks before welding, the intensity of the clamping force, the uniformity of the clamping force, deformation of the clamping beam, flatness error of the based platform and the welding process. A mathematical model is established according to the analysis of misalignment. Experimental results indicate that the model provides an effective theorical guidance in improving welding quality.

Key words: tailored blank laser welding; misalignment; finite element analysis; misalignment prediction modeling

Interfacial structure and properties of galvanized steel sheet joined by pulsed arc brazing process LI Ruifeng, YU Zhishui, HE Jianping (College of Materials Engineering, Shanghai University